Utilizing Quantile Data Envelopment Analysis to Obtain Robust Comparative Performance and Quantile-Based Benchmarking Metrics: Theory and Statistical Properties.

Joseph Atwood[i] and Saleem Shaik[ii]

April 30, 2019

Abstract

This research proposes Quantile Data Envelopment Analysis (qDEA) as a procedure that accounts for the sensitivity of Data Envelopment Analysis (DEA) to data or firm outliers when using DEA to estimate comparative efficiency or benchmarking performance metrics. The qDEA methodology endogenously identifies the distance to a *qDEA-α hyperplane* while allowing up to proportion $q = 1 - \alpha$ of the data observations to lie external to the *qDEA-α hyperplane*. The ability of qDEA to provide more conventional informative quantile-based benchmarking information is discussed. The statistical properties of the qDEA estimator are examined utilizing nCm subsampling and Monte Carlo procedures. Monte Carlo simulations indicate that qDEA distance estimates share the desirable root-n convergence and large sample normality properties of the robust Free Disposal Hull (FDH) based order-m and order-α estimators.

Keywords: *Benchmarking, Data envelopment analysis, Partial moments, Quantile DEA, Robust DEA estimator.*

[i] Corresponding Author; Mailing Address: 309 E Linfield Hall, Department of Agricultural Economics and Economics; Montana State University, P.O. Box 172920; Bozeman, MT 59717-2920, Tel: (406) 994-5614 and Fax: (406) 994-4838, MT. E-mail: jatwood@montana.edu

[ii] Mailing Address: 504 Barry Hall, Department of gribusiness & Applied Economics; North Dakota State University, Dept 7610, PO Box 6050; Fargo, ND 58108-6050, Tel: (701) 231-7459. E-mail: Saleem.Shaik@ndsu.edu

1. Introduction/Motivation

Data Envelopment Analysis (DEA) has proven to be a useful procedure for constructing comparative performance metrics in situations where entities or DMUs are engaged in processes that transform sets of broadly defined inputs into sets of broadly defined outputs. DEA is increasingly being utilized in benchmarking and regulatory applications (Adler, Liebert, and Yazhemsky (2013); Banker, Førsund, and Zhang (2017); Bogetoft and Otto (2011); Bogetoft (2012); Bottasso and Conti (2011); Zanella, Camanho, and Dias (2013)). In regulatory applications, a firm whose "inputs" are too high or "outputs" too low relative to results obtained by other firms in a reference group may be given a period of time to make improvements in their current input-output mix or face financial penalties. In general benchmarking applications, a given decision making unit (DMU) may wish to compare their input-out mix to the levels obtained by other DMUs and attempt to identify potential changes in their operation that might be technically "obtainable" or "reachable" in the short, intermediate, or long-run. In both cases, a reference set of observed input-output realizations from other DMUs is used to construct a set of potential input-output combinations that might be technically "reachable" by the given DMU.

A complication with using DEA in a regulatory or benchmarking setting is the well-known sensitivity of DEA to data outliers. For the purposes of this paper, we define data outliers as either statistical anomalies or data from "outlier" DMUs whose observed input-output levels are not practically "reachable" by a given DMU. Concerns with the sensitivity of distance metrics to statistical outliers has led to the development of procedures to identify and delete potential outliers (Bogetoft and Otto (2011); Simar (2003); Wilson (1993); Wilson (1995)) as well as the development of more robust estimators including the Free Disposal Hull (FDH) based order-m and order-α estimators (Aragon, Daouia and Thomas-Agnan (2005); Cazals, Florens, and Simar (2002); Daouia and Simar (2005); Daouia and Simar(2007a); Daouai and Simar (2007b); Wheelock and Wilson(2008)).

Concerns with the practical "reachability" of points on DEA efficient frontiers has led to the use of clustering procedures where DMU's are compared only to sets of DMU's with similar characteristics (Cook, Ruiz, Sirvent, and Zhu (2017); Dai and Kuosmanen (2014)) or to procedures that endogenously identify directions to points that lie on the efficient DEA frontier but are "closer" or "closest" to a given DMU's data point. (Aparicio, Cordero, and Pastor (2017); Aparicio,

and Pastor (2014); Aparicio, Ruiz, and Sirvent (2007); Ramón, Ruiz, and Sirvent (2018); Ruiz and Sirvent (2016)). Even when a closest frontier point generated by "efficient points" is identified, concerns over the "reachability" of such points has led some researchers to suggest procedures where sets of efficient points are iteratively deleted and the closest projected points generated with the remaining sets of data (Ramón, Ruiz, and Sirvent (2018)). Ramon, Ruiz, and Sivent cite several papers that iteratively eliminate efficient points including a paper by Barr, Durchholz, and Seiford (2000) where the process is termed "peeling the onion."

The sensitivity of comparative performance metrics to data outliers is not unique to DEA. Any comparative study will be sensitive to outliers if a given DMU's performance is contrasted to the performance of the highest one or two achievers within a set of realized outcomes. Recognizing this potential, it is common practice in conventional benchmarking applications (Boxwell (1994); Risk Management Association (2019)) to contrast a given DMU's performance metrics to metrics constructed from a quantile of the population such as the top five, ten, 25 or even 50 percent of DMUs in the industry rather than to the top one or two historically performing DMUs.

The use of quantile benchmarking is desirable in that it decreases the sensitivity of the performance comparisons to statistical outliers and also allows a given firm to compare itself to different "peers" in situations where the performance levels of the "top DMUs" may not be viewed as attainable or "reachable" due to unobserved firm-specific constraints. Quantile-based comparisons provide useful information to a given DMU in that a "bench-mark" may be viewed as more obtainable or "reachable" if 10 percent or more of a group of DMUs have achieved or exceeded the "benchmark" than if only one or two "exceptional" DMUs have attained the standard.

While quantile-based benchmarking is a common practice for more conventional performance metrics, procedures for implementing quantile-based bench marking with DEA are more difficult - especially when the analyst wishes to simultaneously identify sets of more than one potentially "outlying" firms. Order-m and order-α quantile-based estimators have been developed under Free Disposal Hull (FDH) assumptions (Cazals, Florens, and Simar (2002); Daouia and Simar (2005); Daouia and Simar (2007); Daraio and Simar (2007); Wheelock and Wilson (2008)) but quantile estimators have not been commonly available with linear programming based DEA.

Atwood and Shaik (2018) recently introduced the linear programming quantile DEA (qDEA) procedure. Quantile DEA distance metrics are obtained by computing the distance in a given direction from a given DMU's data point to an endogenously identified hyperplane we term the "*qDEA-α hyperplane*". The *qDEA-α* hyperplane divides input-output space into the "*qDEA-α*" and "*qDEA-q*" half-spaces where the *qDEA-α* half-space (in union with the *qDEA-α* hyperplane) contains at least proportion α of the reference set's observed input-output data and the *qDEA-q* half-space contains the remaining proportion $q = 1-\alpha$ of the reference set's observed data. We refer to points lying in the qDEA-*q* half-space as being "external to" the qDEA-α hyperplane and points lying in the qDEA-α half-space as being "internal to" the qDEA-α hyperplane. The qDEA process allows the user to obtain more robust DEA distance metrics by allowing endogenously identified sets of reference observations to lie external to the qDEA-α hyperplane. The conventional DEA process can be viewed as a special case of qDEA in which $q = 0$ or $\alpha = 1$ and no observed data points are allowed to be external to the qDEA-1 hyperplane.

A One-Input One-Output Example

To motivate and illustrate the qDEA concept, we demonstrate the implementation of the qDEA procedure using a modification of Cooper, Seiford, and Tone's (2007, page 26) Constant-Returns-to-Scale (CRS) single-input (employees) single-output (sales) eight DMU example. Given that the traditional DEA input and output orientation results can be obtained as special cases of the Directional DEA (DDEA) (Chambers, Chung, and Färe (1996)) model, all mathematical results and examples in the following discussion will utilize DDEA. Figure 1 reproduces CST's figure 2.1 where the input-output mix for point B has been changed to a more extremal value of (X, Y) = (3,4).

Figure 1 plots the modified CST input/output points. When no points are allowed to lie external to the qDEA hyperplane, the resulting CRS qDEA-1 hyperplane for all DMU's is the red line defined by the origin and point B. If one external point is allowed ($\alpha = 7/8$), the qDEA model endogenously chooses to allow point B to lie external to the hyperplane with the resulting qDEA-(7/8) hyperplane for all DMU's being the black line defined by the origin and point E. If two external points are allowed ($\alpha = 6/8$), the qDEA model endogenously chooses to allow points B and E to lie external to the hyperplane with the resulting qDEA-(6/8) hyperplane for all DMU's

being the blue line defined by the origin and point D. We return to this example below as we present procedures enabling the identification of the qDEA-α hyperplanes in figure 1.

Figure 1: Cooper, Seiford, and Tones Single-Input Single Output Example with DDEA Directions and qDEA CRS Hyperplanes

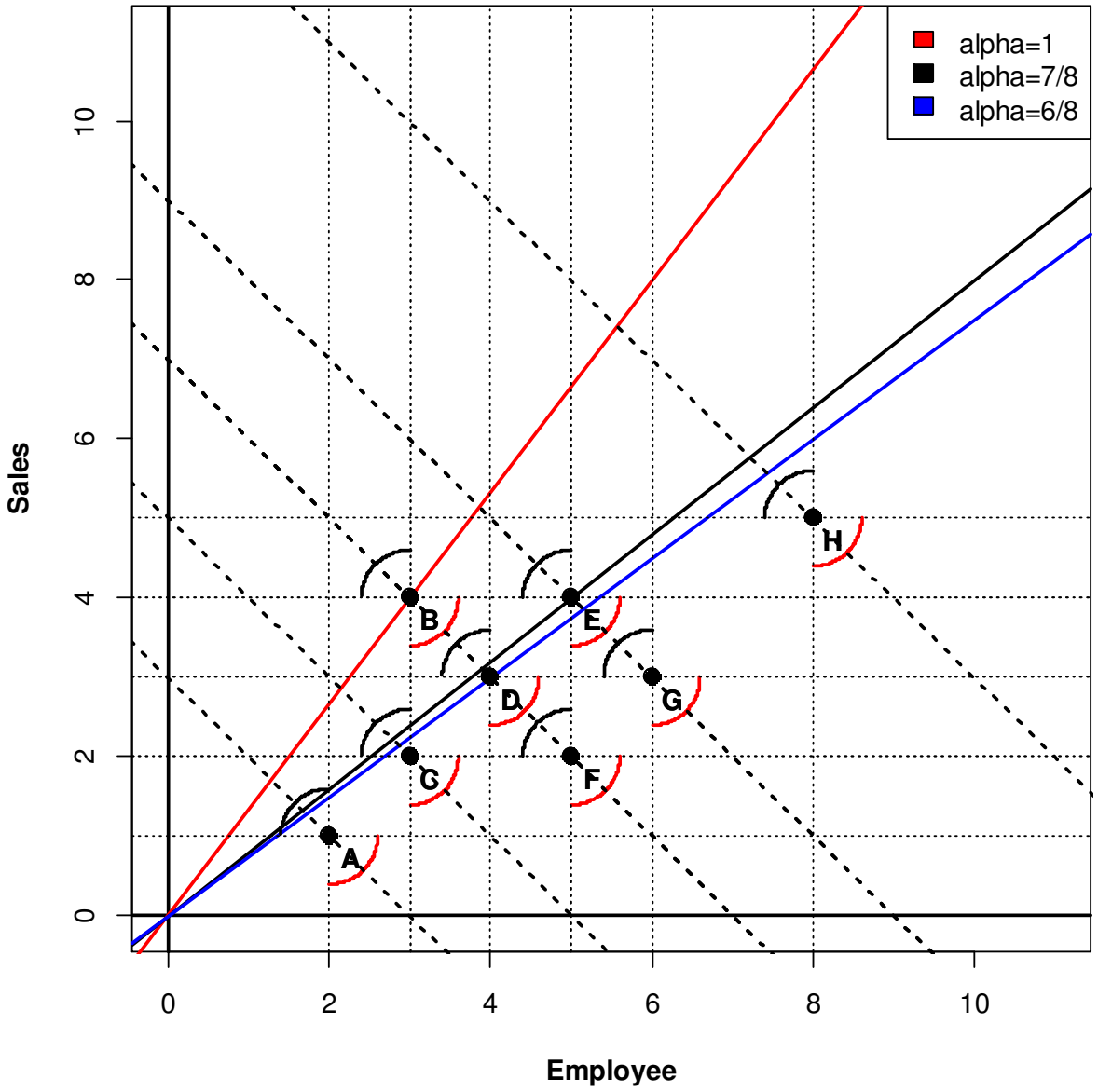

Overview of Paper

Atwood and Shaik (2018)'s chapter did not discuss the statistical properties of the qDEA estimator and several other aspects and limitations of qDEA. In this paper, we examine the qDEA methodology in more detail. We present additional theory involved with the two-stage qDEA

modelling approach including an examination of the conservative solutions commonly resulting from qDEA's use of a stochastic inequality in identifying sets of potential qDEA-α external DMU's. We present an iterative approach to eliminating the conservativeness introduced by the use of the stochastic inequality. We then examine the qDEA estimator's desirable statistical properties of apparent root-n convergence and asymptotic normality. A discussion of caveats and potential future research concludes the paper.

In the following, we specifically: (1) review a conventional primal and dual DDEA model that allows sets of one or more points to lie external to a qDEA-α hyperplane, (2) review a partial moment stochastic inequality and its application in augmented LP models where endogenously identified sets of the original LP constraints are allowed to be violated, (3) review the development of the qDEA model using the partial moment inequality, (4) present a set of small MS-Excel LP examples that implement qDEA using the modified example data from Cooper, Seiford, and Tone (2007) and illustrate the solution conservativeness discussed above, and (5) present the results of a set of simulations examining the statistical properties of the qDEA estimator.

2. Accommodating Sets of "External" Points in a DDEA Model

A primal DDEA model that accommodates potential super-efficiency for DMU-0 with V outputs, U inputs, n reference DMU's, and constant returns to scale (CRS) can be mathematically described as:

$$Max\ \phi$$

$$s.t.$$

$$(1)\quad (a)\quad \sum_{j=1}^{n} y_v^j z_j - d_v^0 \phi \geq y_v^0 \ for\, v = 1,\cdots,V$$

$$(b)\quad \sum_{j=1}^{n} x_u^j z_j + d_u^0 \phi \leq x_u^0 \ for\, u = 1,\cdots,U$$

$$(c)\quad z_j \geq 0 \ for\ j = 1,\cdots,n;\ \phi\ free$$

where ϕ is the directional distance for DMU-0, y_v^j and x_u^j are observed levels of output v and input u for DMU j, d_v^0 and d_u^0 are DMU-0's output v and input u directions, y_v^0 and x_u^0 are DMU-0's observed levels for output v and input u, and z_j is a projection weight assigned to

reference DMU j. We assume that y_v^j and x_u^j are "goods" for all j, v, and u implying that the DDEA directions d_v^0 and d_u^0 are non-negative.

Specifying ϕ as a free variable with $d_v^0 \geq 0$ and $d_u^0 \geq 0$ allows movement in both the "northwest" and "southeast" directions indicated by the black and red arcs in figure 1. If $\phi^{j,\alpha} < 0$ [i], DMU j's data point is "α-superefficient" indicating movement in a "red arc" direction is required to reach DMU j's qDEA-α hyperplane. In general, a qDEA distance $\phi^{j,\alpha} < 0$, $\phi^{j,\alpha} = 0$, and $\phi^{j,\alpha} > 0$ indicates that DMU j's data point is external to (superefficient), on (efficient), or internal to (inefficient) its qDEA-α hyperplane. Figure 1 plots the feasible direction arcs for DMU's A-H. In the following discussion, we report the estimated CRS $\hat{\phi}^{j,\alpha}$ distances for movements in horizontal ("input"), vertical ("output"), and "one-one" directions indicated by the dashed lines in figure 1.

In developing q-DEA, we utilize Charnes, Cooper, and Rhodes' (1978) dual LP approach. The dual linear program of system (1) can be written as:

$$Min \sum_{v=1}^{V} -y_v^0 \; p_v + \sum_{u=1}^{U} x_u^0 \, w_u$$

s.t.

(2) (*a*) $\sum_{v=1}^{V} y_v^j \, p_v - \sum_{u=1}^{U} x_u^j \, w_u \leq 0 \; for \; j = 1, \cdots, n$

(*b*) $\sum_{v=1}^{V} d_v^0 \, p_v + \sum_{u=1}^{U} d_u^0 \, w_u = 1$

(*c*) $p_v \geq 0 \; for \; v = 1, \cdots, V \; ; \;\; w_u \geq 0 \;\; for \; u = 1, \cdots, U$

where the dual values p_v and w_u are CST output and input "prices". We note that if the analyst knew the set of qDEA-α external points a-priori, $\hat{\phi}_n^{\alpha}$ distance estimates could be obtained by deleting observations from system (1) or constraints from inequalities (2a). Alternatively, $\hat{\phi}_n^{\alpha}$ estimates could be obtained by solving system (1) with set of "large" negative "Big-M" values placed in the corresponding primal z_j objective function locations or a set of large positive "Big-M" values placed in the corresponding right-hand-side locations in system (2-a). As it is unlikely that the appropriate set of superefficient points are known a-priori, we present linear programming procedures that can endogenously identify sets of qDEA-α external points.

3. *A Partial Moment Stochastic Inequality, and Its Application in LP Models When Proportional Sets of the LP Constraints Are Allowed to Be Violated*

To endogenously identify a set of qDEA-α external points, we modify the probabilistically constrained linear programming problem presented by Atwood, Watts, Helmers, and Held (1988). AWHH's procedures are broadly applicable in linear programs where the analyst wishes to allow a pre-specified proportion of endogenously identified constraints to be violated. This is accomplished by utilizing the partial moment stochastic inequality presented by Atwood (1985). In the following section, we review Atwood's partial moment inequality and its incorporation in AWHH's probabilistically constrained LP problem.

Partial Moment Stochastic Inequalities

Partial moments can be defined as:

$$(3) \qquad \rho_{LPM}(\gamma,t)=\int_{-\infty}^{t}(t-x)^{\gamma}f(x)\,dx \text{ and } \rho_{UPM}(\gamma,t)=\int_{t}^{\infty}(x-t)^{\gamma}f(x)\,dx \text{ for any } \gamma>0.$$

where $\rho_{LPM}(\gamma,t)$ is a "Lower Partial Moment" (LPM), $\rho_{UPM}(\gamma,t)$ is an "Upper Partial Moment" (UPM), x is a random variable, and *f(x)* is a density function. Mean-Partial Moment models are discussed in the finance literature (Anthonisz (2012); Bawa (1975); Bawa and Lindenberg (1977); Cumova and Nawrocki (2014); Nawrocki (2006); Zhu, Li, and Wang (2009)) as alternatives to Markowitz's (1952) mean-variance criterion. Fishburn (1977) discussed several properties of LPMs including the relationship between mean-LPM efficient solutions and differing degrees of stochastic dominance. Berck and Hihn (1982) presented a stochastic inequality using semivariance (i.e. $\rho_{LPM}(2,\mu_x)$ or $\rho_{UPM}(2,\mu_x)$) and demonstrated that their semivariance based inequality often gave less conservative probability bounds than the one-sided Chebychev inequality. Atwood (1985) generalized Berck and Hihn's (BH) semivariance stochastic inequality using the LPM. The LPM stochastic inequality is derived via:

$$\rho_{LPM}(\gamma,t) = \int_{-\infty}^{t} (t-x)^{\gamma} f(x)\,dx = \int_{-\infty}^{g} (t-x)^{\gamma} f(x)\,dx + \int_{g}^{t} (t-x)^{\gamma} f(x)\,dx \Rightarrow$$

$$\rho_{LPM}(\gamma,t) \geq \int_{-\infty}^{g} (t-x)^{\gamma} f(x)\,dx \geq \int_{-\infty}^{g} (t-g)^{\gamma} f(x)\,dx = (t-g)^{\gamma} \int_{-\infty}^{g} f(x)\,dx \Rightarrow$$

$$\rho_{LPM}(\gamma,t) \geq (t-g)^{\gamma} F(g) \Rightarrow$$

(4) $\text{Prob}(x \leq g) \leq \dfrac{\rho_{LPM}(\gamma,t)}{(t-g)^{\gamma}}$ for all $t > g$ and $\gamma > 0$.

The preceding results use Fishburn's lower partial moment but can easily be modified to the use of upper partial moments (UPM) when computing limits on the probability of upside events. With the UPM and setting $g > t$, similar manipulations give:

(5) $\text{Prob}(x \geq g) \leq \dfrac{\rho_{UPM}(\gamma,t)}{(g-t)^{\gamma}}$ for all $g > t$ and $\gamma > 0$.

The PM inequalities are interesting results that (with an appropriate choice of γ and t) will usually generate less conservative upper bounds than a one-sided Chebychev inequality $\text{Prob}(\mu - k\sigma \leq g) \leq \left(\dfrac{1}{1+k^2}\right)$ or the BH semi-variance inequality $\text{Prob}(x \leq \mu - k\rho_{LPM}(2,\mu)) \leq \left(\dfrac{1}{k^2}\right)$.

Figure 2 illustrates these results by plotting stochastic inequality probability bounds on the probability of x falling below g = 60 with x~Normal (100, 25). Figure 2 plots the probability bounds for the one-sided Chebychev inequality as well as the LPM based $\dfrac{\rho(\gamma,t)}{(t-g)^{\gamma}}$ probability limits for various combinations of γ and t. Figure 2 also contrasts the probability bounds to the actual probability pnorm (60, mean = 100, sd = 25) ~0.055. The BH semivariance probability bound is the right-most point on the red curve and is less conservative than the Chebychev one-tailed limit. For each γ, less conservative LPM-based probability bounds can be found depending upon the level of t but an inappropriate level for t may also generate excessively conservative probability bounds. In situations where the Chebychev or the BH inequality bounds are exact, the LPM inequality will generate exact probability bounds for an appropriate choice of t and γ.

The linear partial moment inequality $(\gamma = 1)$ can often generate less conservative bounds than using higher order partial moments. We limit our discussion to the set of linear partial moments as the linear partial moment can be computed in an LP model modeled with a finitely discrete set of

outcomes. Atwood (1985) and AWHH (1988) demonstrated that, with a linear PM, a given

Figure 2: Lower Partial Moment (LPM) Probability Bounds

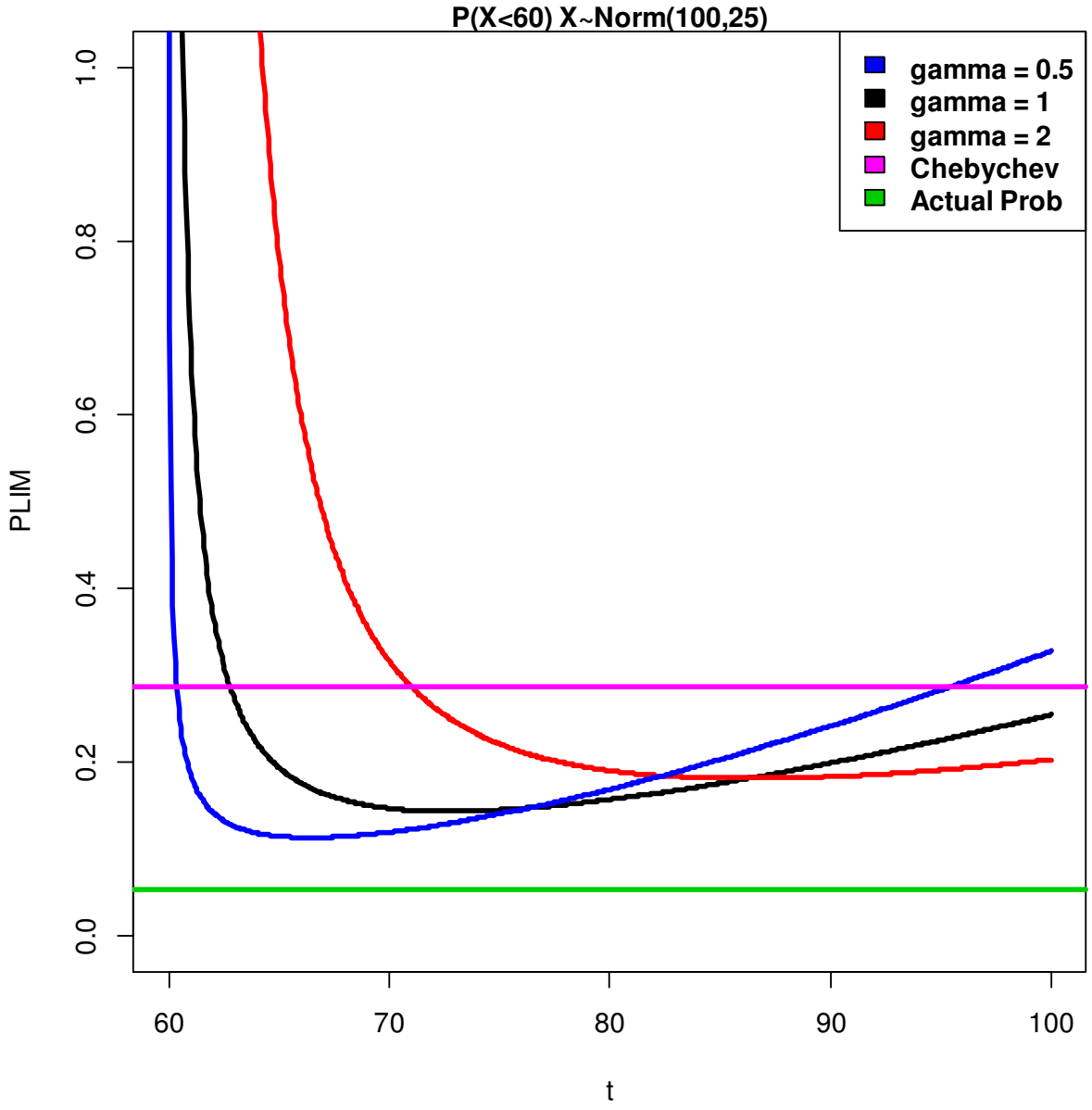

application's least conservative level for t could be endogenously determined in a linear programming model. Denoting the linear partial moments as $\rho_{LPM}(1,t) = \rho_{LPM}(t)$ and $\rho_{UPM}(1,t) = \rho_{UPM}(t)$, we can rewrite the probability limits (4) and (5) as:

(6) $\text{Prob}(x \le g) \le \dfrac{\rho_{LPM}(t)}{(t-g)>0}$ and $\text{Prob}(x \ge g) \le \dfrac{\rho_{UPM}(t)}{(g-t)>0}$.

Enforcing constraints:

(7) $t - {}^{1}\!/_{q}\,\rho_{LPM}(t) \ge g$ and $\rho_{LPM}(t) \ge 0$

or

(8) $t + {}^{1}\!/_{q}\,\rho_{UPM}(t) \le g$ and $\rho_{UPM}(t) \ge 0$

while allowing the LP model to endogenously determine the least constraining partial moment limit $\tilde{t}$ and compute the linear partial moments $\rho_{LPM}(\tilde{t})$ or $\rho_{UPM}(\tilde{t})$ is sufficient to guarantee that

$$\text{Prob}(x \le g) \le \frac{\rho_{LPM}(\tilde{t})}{(t-g)>0} \le q \text{ or } \text{Prob}(x \ge g) \le \frac{\rho_{UPM}(\tilde{t})}{(g-t)>0} \le q .$$

AWHH utilized the linear LPM inequality results in constructing a model that maximized the expected income of a portfolio of assets subject to a set of technical constraints and the additional requirement that the probability of income falling below a target level g not exceed q. Modifying their notation slightly, AWHH's portfolio optimization model with J assets, I portfolio constraints, and K states of nature can be written as:

$$\underset{z}{Max}\ \mu_x = \sum_{j=1}^{J} \mu_{z,j}\, z_j$$

$$s.\text{t.}$$

$$(a) \quad \sum_{j=1}^{J} a_{i,j}\, z_j \le b_i \quad i = 1,\cdots,I$$

(9)

$$(b) \quad \sum_{j=1}^{J} y_{k,j}\, z_j - t + \delta_k \ge 0 \quad k = 1,\cdots,K$$

$$(c) \quad \sum_{k=1}^{K} r_k\ \delta_k - \rho_{LPM} = 0$$

$$(d) \quad t - \frac{1}{q}\rho_{LPM} \ge g$$

$$(e) \quad z_j \ge 0 \text{ for } j = 1,\cdots J;\ t \text{ free};\ \delta_k \ge 0;\quad \rho_{LPM} \ge 0$$

where $x_k = \sum_{j=1}^{J} y_{k,j}\, z_j$ is portfolio income in state k, μ_x is the mean portfolio income, $\mu_{z,j}$ is asset j's mean income, z_j is the chosen level of asset j, $a_{i,j}$ and b_i are portfolio constraint coefficients, $y_{k,j}$ is the return to asset j in state k, t is an endogenously determined linear LPM integral limit, δ_k is an income deviation below level t with $\delta_k = t - \sum_{j=1}^{J} y_{k,j}\ z_j = t - x_k$ when $x_k <$ t and zero otherwise, r_k is a non-negative "probability" of state k satisfying $\sum_{k=1}^{K} r_k = 1$, $\rho_{LPM} = \rho_{LPM}(t)$ is the

endogenously computed linear LPM, and g is a level of income that must be exceeded with probability $\alpha = 1 - q$. System (9) selects a vector of optimal portfolio levels $\tilde{z}$ that map to a vector of potential portfolio income realizations $\tilde{x}$. The model maximizes the portfolio's expected income μ_x subject to technical portfolio constraints and the constraint $\tilde{t} - \frac{1}{q}\rho_{LPM}(\tilde{t}) \geq g$ thus guarantying $\text{Prob}(\tilde{x} \leq g) \leq q$.

The potential income levels $\tilde{x}$ chosen in system (9) were found to satisfy the probability constraint but were often found to be excessively "conservative" in that the actual probability of portfolio income falling below g was frequently much lower than q. The reason for this conservativeness can be explained using insights from two reviewers who correctly pointed out that the AWHH's (1988) model is similar to Rockafellar and Urysev (2000)'s conditional Value at Risk (cVaR) model. This perception is correct in that an upside-risk version of system (9) can be shown to be equivalent to a cVaR_q constrained version of Rockafellar and Urysev's (RU) model[ii]. With an upside risk model of losses, Rockafellar and Urysev's proofs imply that the optimal $\tilde{t}$ and g terms in the binding upside risk constraint $\tilde{t} + \frac{1}{q}\rho_{UPM}(\tilde{t}) = g$ are, respectively, the solution's q-level "Value at Risk" (VaR_q) and the associated "conditional Value at Risk" (cVaR_q) [iii]

The "conservativeness" of system (9)'s solutions arises from the common result that $g < \tilde{t}$ or $\text{cVaR}_q(\tilde{x}) < \text{VaR}_q(\tilde{x})$. System (9) actually guarantees that $\text{Prob}(\tilde{x} \leq \tilde{t}) \leq q$ with $\text{Prob}(\tilde{x} \leq g)$ usually being less than q, i.e. "conservative". There are several possible approaches to obtaining less conservative solutions than those obtained from system (9). Subsequent unpublished research suggested that a two-stage process where the first stage (system (9)) is used to identify constraints (constraints with $\delta_k > 0$) to be "relaxed" in a second stage would generate less conservative outcomes.

In the following we utilize a two-stage process[iv] where, in Stage 1, an augmented dual-DDEA system similar to system (9) is utilized to identify constraints to be relaxed (i.e. identify sets of potential qDEA-α super-efficient DMUs). Stage 2 of qDEA consists of solving conventional DDEA models (1) or (2) with the constraints identified in qDEA Stage-1 being relaxed. Given that

constraints (2-a) is system (2) involve "$\leq$ restrictions", we utilize the upper partial moment $\rho_{UPM}(t)$ and the $t + \frac{1}{q}\rho_{UPM}(t) \leq g$ sufficiency constraint.

4. The qDEA Model

Dual DDEA system (2) is augmented to implement the first stage of the qDEA model as follows:

$$
\begin{aligned}
& Min \sum_{v=1}^{V} -y_v^0 \; p_v + \sum_{u=1}^{U} x_u^0 \, w_u \\
& s.t. \\
& (a) \quad \sum_{v=1}^{V} y_v^j \; p_v \; - \sum_{u=1}^{U} x_u^j \, w_u - t - \delta_j \leq 0 \;\text{ for }\; j = 1, \cdots, n \\
& (b) \quad \sum_{v=1}^{V} d_v^0 \; p_v \; + \sum_{u=1}^{U} d_u^0 \, w_u \; = 1 \\
& (c) \quad \sum_{j=1}^{n} \frac{1}{n} \, \delta_j \; - 1 \rho_{UPM} \; = 0 \\
& (d) \quad 1t \; + \; \frac{1}{q} \rho_{UPM} \leq 0 \\
& (e) \quad p_v \geq 0; \; w_u \geq 0; \; t \text{ a free variable}; \; \delta_j \geq 0; \; \rho_{UPM} \geq 0
\end{aligned}
\qquad (10)
$$

where p_v is an output "price", w_u is an input "price", t is the endogenously determined upper partial moment (UPM) "integral" limit, δ_j is a deviation above t when $\sum_{v=1}^{V} y_v^j \; p_v \; - \sum_{u=1}^{U} x_u^j \, w_u > t$ and zero otherwise, $\rho_{UPM} = \rho_{UPM}(t)$ is the endogenously calculated linear UPM, and $0 < q < 1$ is the maximal proportion of data points that are allowed to lie outside the qDEA-α hyperplane. Since we wish to allow up to proportion *q* of the constraints in system (2-a) to be violated, we set g = 0 in the UPM constraint (10-d) and allow *t* to be negative. System (2) is fully nested in system (10) as setting $q < 1/n$ will guaranty that no points can lie outside the hyperplane thus obtaining the conventional DDEA results.

Potential qDEA-α super-efficient DMU's or external points in system (10) are identified as constraints with positive δ_j values in the solution. System (10) may sometimes be conservative in that fewer than proportion *q* of the δ_j may be positive but the solutions to system (10) will have no more than proportion *q* of potentially external points. We also demonstrate below that the objective function value from expression (10) does not give the final DDEA distance estimate as

system (10)'s "extrapolated point" (and the resulting distance metric) will consist of an extrapolation using information from all "external" points plus the new qDEA "support points"[v]. While system (10) generates conservative distance estimates, the set of positive δ_j values endogenously identifies a set of *potential points* allowed to lie external to the given DMU's qDEA-α hyperplane. The second stage of the qDEA process re-estimates system (2) while relaxing the constraints associated with the potential external points identified in stage-1.

5. qDEA Application and Implementation

In this section, we develop q-DEA estimates for our modification of Cooper, Sieford, and Tone's (CST) eight DMU example. The input (employees) and output (sales) data, estimated qDEA-α distances, and "projected points" are presented in table 1. Table 1 presents the qDEA constant returns to scale (CRS) results using three directional assumptions: (a) the input orientation problem or horizontal movement with directions $(d_u^j = x_u^j,\ d_v^j = 0)$, (b) the output orientation problem or vertical movement with directions $(d_u^j = 0,\ d_v^j = y_v^j)$, and (c) a unit or "one-one" direction model with diagonal directions $(d_u^j = 1,\ d_v^j = 1)$ while allowing 0, 1, or 2 points to lie external to the qDEA-α hyperplane.

The qDEA solution to this problem is obtained in two stages. Figures 3 and 4 illustrate the implementation of qDEA for DMU H using screen shots from MS-Excel. Figure 3 presents an augmented MS Solver tableau for qDEA stage-1 (system (10)) while allowing no more than two points to lie external to the hull. From our experience with the conservative partial moment models, if we want no more than NP = 2 points to lie external to the hull, identifying the positive δ_j values are less sensitive to rounding errors (for small δ_j positive values) if q is set just below (NP+1)/n. For this problem with NP = 2, q was set equal to (2+1) / 8 - 0.0001 = 3/8 - 0.0001 = 0.37499 which will guarantee that the proportion of the positive δ_j will not exceed 0.37499 < 3/8. The value 1/q in the constraint matrix is thus 1/0.37499 ~2.6667. The highlighted qDEA stage-1 solution in figure 3 indicates that the model has determined to allow points B and E to ***potentially lie*** external to the qDEA-(6/8) hyperplane. The objective value from qDEA stage-1 is a

Table 1: Modified CST Example -- Input-Output Levels, CRS DDEA and qDEA Distances and Projected Points For One and Two External Points

			NO EXTERNAL POINTS			ONE EXTERNAL POINT			TWO EXTERNAL POINTS		
			INPUT ORIENTATION								
			DISTANCE	PROJECTED VALUES		DISTANCE	PROJECTED VALUES		DISTANCE	PROJECTED VALUES	
DMU	x	y	$\hat{\phi}^{j}$	$\tilde{x}$	$\tilde{y}$	$\hat{\phi}^{j,7/8}$	$\tilde{x}$	$\tilde{y}$	$\hat{\phi}^{j,6/8}$	$\tilde{x}$	$\tilde{y}$
A	2	1	0.625	0.75	1.00	0.375	1.25	1.00	0.333	1.33	1.00
B	3	4	0.000	3.00	4.00	-0.667	5.00	4.00	-0.778	5.33	4.00
C	3	2	0.500	1.50	2.00	0.167	2.50	2.00	0.111	2.67	2.00
D	4	3	0.437	2.25	3.00	0.062	3.75	3.00	0.000	4.00	3.00
E	5	4	0.400	3.00	4.00	0.000	5.00	4.00	-0.067	5.33	4.00
F	5	2	0.700	1.50	2.00	0.500	2.50	2.00	0.467	2.67	2.00
G	6	3	0.625	2.25	3.00	0.375	3.75	3.00	0.333	4.00	3.00
H	8	5	0.531	3.75	5.00	0.219	6.25	5.00	0.167	6.67	5.00
			OUTPUT ORIENTATION								
			DISTANCE	PROJECTED VALUES		DISTANCE	PROJECTED VALUES		DISTANCE	PROJECTED VALUES	
DMU	x	y	$\hat{\phi}^{j}$	$\tilde{x}$	$\tilde{y}$	$\hat{\phi}^{j,7/8}$	$\tilde{x}$	$\tilde{y}$	$\hat{\phi}^{j,6/8}$	$\tilde{x}$	$\tilde{y}$
A	2	1	1.667	2.00	2.67	0.600	2.00	1.60	0.500	2.00	1.50
B	3	4	0.000	3.00	4.00	-0.400	3.00	2.40	-0.437	3.00	2.25
C	3	2	1.000	3.00	4.00	0.200	3.00	2.40	0.125	3.00	2.25
D	4	3	0.778	4.00	5.33	0.067	4.00	3.20	0.000	4.00	3.00
E	5	4	0.667	5.00	6.67	0.000	5.00	4.00	-0.062	5.00	3.75
F	5	2	2.333	5.00	6.67	1.000	5.00	4.00	0.875	5.00	3.75
G	6	3	1.667	6.00	8.00	0.600	6.00	4.80	0.500	6.00	4.50
H	8	5	1.133	8.00	10.67	0.280	8.00	6.40	0.200	8.00	6.00
			ONE-ONE ORIENTATION								
			DISTANCE	PROJECTED VALUES		DISTANCE	PROJECTED VALUES		DISTANCE	PROJECTED VALUES	
DMU	x	y	$\hat{\phi}^{j}$	$\tilde{x}$	$\tilde{y}$	$\hat{\phi}^{j,7/8}$	$\tilde{x}$	$\tilde{y}$	$\hat{\phi}^{j,6/8}$	$\tilde{x}$	$\tilde{y}$
A	2	1	0.714	1.29	1.71	0.333	1.67	1.33	0.286	1.71	1.29
B	3	4	0.000	3.00	4.00	-0.889	3.89	3.11	-1.000	4.00	3.00
C	3	2	0.857	2.14	2.86	0.222	2.78	2.22	0.143	2.86	2.14
D	4	3	1.000	3.00	4.00	0.111	3.89	3.11	0.000	4.00	3.00
E	5	4	1.143	3.86	5.14	0.000	5.00	4.00	-0.143	5.14	3.86
F	5	2	2.000	3.00	4.00	1.111	3.89	3.11	1.000	4.00	3.00
G	6	3	2.143	3.86	5.14	1.000	5.00	4.00	0.857	5.14	3.86
H	8	5	2.429	5.57	7.43	0.778	7.22	5.78	0.571	7.43	5.57

Figure 3: qDEA Stage-1 Tableau Identifying Two Potential External Points

							qDEA STAGE 1									
MODIFIED CST EXAMPLE			SELECTED				N out =	2								
DUAL PROBLEM			DMU =	H			*q* =	0.375								
DMU	OUTPUT	INPUT	T	D-A	D-B	D-C	D-D	D-E	D-F	D-G	D-H	T-LPM		LHS	SIGN	RHS	DUALS
A	1	-2	-1	-1	0	0	0	0	0	0	0	0		-0.08695	<=	0	0
B	4	-3	-1	0	-1	0	0	0	0	0	0	0		0.00000	<=	0	-0.5652
C	2	-3	-1	0	0	-1	0	0	0	0	0	0		-0.04348	<=	0	0
D	3	-4	-1	0	0	0	-1	0	0	0	0	0		0.00000	<=	0	-0.5652
E	4	-5	-1	0	0	0	0	-1	0	0	0	0		0.00000	<=	0	-0.5652
F	2	-5	-1	0	0	0	0	0	-1	0	0	0		-1.00000	<=	0	0
G	3	-6	-1	0	0	0	0	0	0	-1	0	0		-0.95652	<=	0	0
H	5	-8	-1	0	0	0	0	0	0	0	-1	0		-0.86957	<=	0	0
DIRECTION	1	1	0	0	0	0	0	0	0	0	0	0		1.00000	==	1	1.21741
LPM CALC	0	0	0	0.125	0.125	0.125	0.125	0.125	0.125	0.125	0.125	-1		0.00000	==	0	-4.5218
QRESTRICT	0	0	1	0	0	0	0	0	0	0	0	2.6667		0.00000	<=	0	-1.6956
OBJ	-5	8	0	0	0	0	0	0	0	0	0	0		1.217407	<--minOBJ		
												NOTE THIS OBJ IS NOT THE FINAL ANSWER					
												STAGE 2 PROVIDES THE FINAL ANSWER					
	t-lower bound		-1000														
														PROJECTED POINTS			
	P	W	T	D-A	D-B	D-C	D-D	D-E	D-F	D-G	D-H	T-LPM		$\tilde{x}$	$\tilde{y}$		
SOLUTION	0.52174	0.47826	-0.3478	0	1	0	0	0.0435	0	0	0	0.1304		6.7826	6.2174		

conservative[vi] $\hat{\phi}^H = 1.21741$ with projected point $(\tilde{x}_H, \tilde{y}_H) = \left(x_H - \hat{\phi}^H 1, y_H + \hat{\phi}^H 1\right) = (6.7826,$ 6.2174). The second stage of the qDEA model is a DDEA model (2) with relaxed constraints. Figure 4 presents the qDEA stage-2 dual tableau (system (2)) where the constraints associated with points B and E have been "relaxed". The resulting qDEA-(6/8) direction (1, 1) distance is $\hat{\phi}^{H,6/8} =$ 0.5714 for point H. In figure 4, we relax the constraints associated with DMU's B and E by adding "large" positive values in the corresponding right hand side locations.

Figure 4: QDEA Stage II Tableau Identifying qDEA Efficiency Scores

		qDEA STAGE 2					
MODIFIED CST EXAMPLE			SELECTED				
DUAL PROBLEM			DMU =	H			
DMU	OUTPUT	INPUT		LHS	SIGN	RHS	DUALS
A	1	-2		-0.2857	<=	0	0
B	4	-3		1.0000	<=	1000	0
C	2	-3		-0.1429	<=	0	0
D	3	-4		0.0000	<=	0	-1.8571
E	4	-5		0.1429	<=	1000	0
F	2	-5		-1.0000	<=	0	0
G	3	-6		-0.8571	<=	0	0
H	5	-8		-0.5714	<=	0	0
DIRECTION	1	1		1	==	1	0.5714
OBJ	-5	8		0.5714	<--minOBJ		
				PROJECTED POINTS			
	P	W		$\tilde{x}$	$\tilde{y}$		
SOLUTION	0.571429	0.428571		7.4286	5.5714		

We conclude this section by noting that the figure 4's "left-hand-side" (LHS) values for the constraints associated with both DMU's B and E exceed 0, indicating that points B and E are indeed external to DMU H's qDEA-6/8 hyperplane. We return to this issue below where we

discuss an example where one "iteration" of the two-stage qDEA process does not result in two external points due to the conservativeness of the partial moment inequality[vii].

qDEA Distances for the Modified CST Example

Table 1 presents the DDEA and qDEA distances and projected points for all eight DMU's under constant returns to scale and for the input $\left(d_u^j = x_u^j,\, d_v^j = 0\right)$, output $\left(d_u^j = 0,\, d_v^j = y_v^j\right)$, and diagonal $\left(d_u^j = 1,\, d_v^j = 1\right)$ directions. The $\hat{\phi}^j$ distance scores are the conventional directional distances indicating that only DMU B (with a $\hat{\phi}^j$ distance of zero) is on the CRS DDEA efficient boundary (the red ray in figure 1). When one external point is allowed, the CRS qDEA-(7/8) distances indicate that point B is now "qDEA-(7/8) superefficient" ($\hat{\phi}^{B,7/8} < 0$) while point E becomes qDEA-(7/8) efficient ($\hat{\phi}^{E,7/8} = 0$). The CRS qDEA-(7/8) distances of all other points have decreased by a fairly substantial amount. The super-efficiency of point B and the substantial decrease of the other DMU's qDEA-(7/8) efficiency scores provide evidence that point B is potentially an influential outlying point.

When two external points are allowed, the CRS qDEA-(6/8) scores of all DMU's decrease but by a smaller amount than when the first point was excluded. With two external points, DMUs B and E become qDEA-(6/8) superefficient ($\hat{\phi}^{B,6/8}$ and $\hat{\phi}^{E,6/8} < 0$) while DMU D ($\hat{\phi}^{D,6/8} = 0$) is now on the qDEA-(6/8) efficient.

Table 1 presents the extrapolated points for the DDEA, qDEA-(7/8), and qDEA-(6/8) models and for the "input", "output" and "one-one" directions. From figure 1, we expect points (B, E), points (D, G) and points (C, F) to project or map to the same points on the qDEA hyperplanes with input directions, points (B, C) and points (E, F) to map to the same points with output directions, and (B, D, F) and points (E, G) map to the same points on the DDEA, qDEA-(7/8) and qDEA-(6/8) hyperplanes. The results presented in table 1 confirm these expectations.

We conclude the discussion of the CST example by noting that, if estimated with variable returns to scale (VRS), the qDEA-α hyperplane's external points will often be DMU and direction dependent. As discussed by Atwood and Shaik (2018), with VRS qDEA-α distances *(in some*

directions) for some qDEA-α superefficient DMU's will be dual unbounded (primal infeasible) due to the increased number of points that are allowed to be external to the DMU's qDEA-α hyperplane. For example, in figure 1, with VRS and one external point, points H and A will be qDEA-(7/8) superefficient. Movement in the input (horizontal) direction from point H or the output (vertical) direction from point A will result in a primal infeasibility as movement in those directions cannot reach an endogenously identified qDEA-(7/8) hyperplane.

Although not discussed by Atwood and Shaik, several authors (Chen (2005); Chen and Liang (2011); Cook, Liang, and Zhu (2009); Lee, Chu, and Zhu (2011); Lee, Chu, and Zhu (2012); Lovell and Rouse (2003); Seiford and Zhu (1999)) have proposed methods to allow estimation of DEA metrics for superefficient DMU's whose initial DEA solutions are primal infeasible. Many of the suggested procedures involve the identification of alternative directions that allow movement from the given DMU's input-output observation to a point on a feasible data-generated hyperplane[viii].

6. The "q-Conservativeness" of qDEA Stage-2 Solutions

Another concern with qDEA is that, in practice, we often find that a single iteration of the qDEA two-stage process results in *"q-conservative"* solutions in that fewer than proportion *q* of the data points actually lie external to the qDEA-α hyperplane at the completion of qDEA stage-2. In our experience, conservative stage-2 solutions are more likely if the data contains large influential outliers. The reason for conservative stage-2 solutions lies in the use of the stochastic inequality when identifying *potential* external points in qDEA stage-1. The qDEA stage-1 model allows the LP model to select a partial moment limit t and endogenously contort the original constraint polytope while constraining the weighted sums of deviations above t in such a way that no more than proportion q of the $\delta_j = y^j p - x^j w + t$ values lie above zero. While the solution will commonly have up to proportion *q* of positive δ_j values identifying "potential" external points in the original DEA problem, not all such points may actually be external when the qDEA stage-2 problem is solved. In response to this issue, we developed a multi-iteration procedure that addresses the qDEA stage-2 conservativeness and allows the researcher to identify solutions with proportion q of external points if such a solution is feasible.

An q-conservative example is easily constructed by modifying the above application's DMU B observation to a more extremal $\left(x^B, y^B\right) = (2,5)$ while attempting to allow two external points. At the completion of the procedures demonstrated in figures 3 and 4, we find that only one point actually lies external to the qDEA hyperplane. Supplemental material available from the authors demonstrates a multi-iteration procedure that addresses the issue and identifies two external points. As also discussed in the supplemental material, from our simulation experience it appears that the original distance estimates obtained from completing *and bootstrapping* one iteration of the qDEA process will generate *consistent* estimates of the $\hat{\phi}^{\hat{\alpha}}$ distance where $\hat{\alpha} = 1 - \hat{q}$ and $\hat{q}$ is the proportion of Stage-2's "actual external points". While in many benchmarking exercises one iteration and an estimate of the corresponding $\hat{q}$ may be sufficient, R code available from the authors allows the user to specify the number of two-stage qDEA iterations and the $\hat{q}$ -tolerance desired. All results in the following sections of the paper have been estimated with up to 4 iterations of the two-stage qDEA process described in the supplemental material.

We have presented the qDEA model and demonstrated its ability to obtain quantile distance/efficiency metrics as well as qDEA's ability to identify sets of potentially outlying data points. We now examine the statistical properties of the qDEA estimators.

7. Statistical Properties of qDEA Estimates

A natural question is whether the qDEA estimator possesses desirable statistical properties. Given that, to date, we have not been able to derive closed form expressions for the asymptotic properties of the qDEA estimator, we use several assumed data generating processes (DGP) and numerical methods to examine these properties. Specifically we use Monte Carlo simulations and a slight modification of nCm subsample bootstrapping theory to examine the "large sample" properties of the qDEA estimator. In the next section of the paper, we describe: (1) the procedures utilized to estimate large sample convergence rates and perform normality tests for the qDEA estimates and (2) the class of DGP used in the Monte Carlo simulations. We then present and discuss the results of the large sample convergence rate estimations and normality tests.

Numerically Estimating Large Sample Statistical Properties

Geyer (2013) presents a succinct review of the Politis, Romano, and Wolf's (1999, 2001) nCm subsampling process. Space presents a complete discussion but the results are that confidence intervals for a statistic $\hat{\theta}_n$ can often be estimated by utilizing properties of the statistic:

(11) $S_m = \hat{\theta}_n - \left(\frac{m}{n}\right)^{\beta}\left(\hat{\theta}_m - \hat{\theta}_n\right)$

where $\hat{\theta}_n$ is a parameter estimate obtained from a sample of size n, β is a "convergence rate", and $\hat{\theta}_m$ is an estimate from a subsample of size m(n) $\ll$ n where $\ll$ denotes "much smaller than" [ix]. In finite sample bootstrapping, B sets of m observations are repeatedly resampled from a given sample of size n and used to estimate $\hat{\theta}_{m,b}$ for b = 1,…,B. Confidence intervals for the population parameter θ can then be estimated by using the quantiles of the set of B simulated statistics:

(12) $S_{m,b} = \hat{\theta}_n - \left(\frac{m}{n}\right)^{\beta}\left(\hat{\theta}_{m,b} - \hat{\theta}_n\right)$.

Constructing expression (12)'s $S_{m,b}$ values requires that the analyst identify appropriate levels for both the convergence rate β and the subsample size m. While the convergence rates for the DEA, FDH, and FDH-related order-m and order-α estimators are known[x], we have not been able to derive β for the qDEA estimator.

Given that there is no known way to exogenously select the optimal level for the subsample size m (Politis et. al. (1999)), a common practice is to estimate $\hat{\theta}_{m_i,b}$ over a range of M m_i values and select the appropriate m_i using data driven results (Politis et. al. (1999); Simar and Wilson (2011-b)). When both the DGP and β are unknown, Politis et. al. (1999-chapter 8) and Geyer discuss finite-sample procedures utilizing the bootstrapped $\hat{\theta}_{m,b}$ values to estimate the unknown convergence rate parameter β. Politis et. al. suggest estimating convergence rates by examining the rate at which inter-quantile-ranges computed from $\hat{\theta}_{m_i,b}$ change with increases in the subsample size m_i. We initially utilized their suggested finite sample $\hat{\beta}$ estimation procedures but found that, while the "finite sample" $\hat{\beta}$ estimates performed relatively well as n increased, the procedures gave unstable results at smaller sample sizes such as when n = 100. Due to the

unstable results at smaller sample sizes, we chose to use Monte Carlo procedures to estimate "large sample" convergence rates for a set of *assumed* data generating processes.

When estimating "large sample" convergence rates we use an **assumed** DGP to generate 1000 $\left(X_{N,mcs}, Y_{N,mcs}\right)$ data sets of size N = 20000 for Monte Carlo repetition *mcs* = 1, …,1000. We then estimated $\hat{\phi}^{\alpha}_{m_i,mcs}$ distances for each sample size m_i in a vector of ten subsample sizes in *mlist* ranging between 1000 and 20000. Motivated by one of Geyer's examples, we used the following vector *mlist* of m_i values to estimate large sample convergence rates:

mlist = round(exp(seq(log(1000),log(20000), length.out=10)),0) obtaining *mlist* = (1000, 1395, 1946, 2714, 3786, 5282, 7368, 10278, 14337, 20000) [xi]. We emphasize that since we are repeatedly simulating data from an assumed DGP and estimating only one set of $\hat{\phi}^{\alpha}_{m_i,mcs}$ for each mcs repetition, we are not limited by the $m_i << n$ requirement necessary when repeatedly subsampling from a **given** sample of size n. For each sample size m_i in mlist, $\hat{\phi}^{\alpha}_{m_i,mcs}$ is estimated using the first m_i observations in the data set $\left(X_{N,mcs}, Y_{N,mcs}\right)$. The 1000 sets of $\hat{\phi}^{\alpha}_{m_i,mcs}$ estimates are then stored in a 1000 x 10 matrix "qeffhat".

Given mlist and the qDEA parameter estimates matrix "qeffhat", the estimated convergence rate $\hat{\beta}$ can be estimated using the following R script:

```
 # Estimate convergence parameter betahat
IQNR = function(x) {quantile(x,qU) - quantile(x,qL)}
qL=seq(0.01, 0.24, 0.01)
qU=qL + 0.75
iqnr=as.vector(apply(qeffhat, 2, IQNR))
m=rep(mlist, each = length(qL))
betahat= -1* summary(lm(log(iqnr) ~ log(m)))$coeff[2,1]
```

The above script generates a vector of 24 inter-quantile quantile range (iqnr) estimates for each sample size m_i, pools the iqnr values across sample sizes, matches the iqnr values with the corresponding sample size, and regresses the log of the iqnr against the log of the sample size m_i. The estimated convergence parameter $\hat{\beta}$ is recovered as the regression slope parameter multiplied be a negative one.

We also applied a Pearson normality test of $\hat{\phi}^{\alpha}_{m_i,mcs}$ for each sample size using the following R script:

```
# Test for normality of qDEA estimates by sample size
library(nortest)
pcalc=function(x) {pearson.test(x)$p.value}
pvalues = apply(qeffhat, 2, pcalc)
```

The object *pvalues* contains a vector of Pearson p-values with low values indicating that normality should be rejected.

Data Generating Processes (DGP)

We examined the convergence of the qDEA estimator using Monte Carlo procedures with several assumed data generating processes (DGP). The results presented below used Simar and Wilson's (2011-b) assumed DGP with returns to scale parameters $\lambda = 0.80$ or $\lambda = 1.0$ to generate U = 1, 3, and 5 input and V = 1 output data for a given DMU^0 and also to repeatedly generate input-output reference sets of N = 20,000 reference DMU's. When $\lambda = 0.80$, we estimated the qDEA model with a variable returns to scale (VRS) qDEA model. When $\lambda = 1.0$, the qDEA model was estimated with constant returns to scale (CRS) LP. "Efficient" input and the output levels for DMU^0 were set at $\tilde{x}_u^0 = 0.5$ for u = 1, …U, with $\tilde{y}^0 = \left(\prod_{u=1}^{U} \tilde{x}_u^0 \right)^{\lambda/U}$ giving $\tilde{y}^0 = 0.5$ when $\lambda = 1$ and $\tilde{y}^0 = 0.57435$ when $\lambda = 0.80$. "Inefficiency" is introduced for DMU^0 via setting $x_u^0 = 2\tilde{x}_u^0 = 1$ and $y^0 = \tilde{y}^0$. The corresponding input-orientation DDEA parameter with directions $d_u^0 = x_u^0$ and $d_v^0 = 0$ can be shown to be $\phi = 0.5$.

For each Monte Carlo simulation mcs = 1,…, 1000, a reference DMU data set of size N = 20000 was generated using simulated "efficient" input-output levels generated via: $\tilde{x}^j_{u,mcs} \overset{iid}{\sim} unif(0,1)$ and $\tilde{y}^j_{mcs} = \left(\prod_{u=1}^{U} \tilde{x}^j_{u,mcs} \right)^{\lambda/U}$ for DMUs j = 1,…, N. Input "inefficiency" for DMU^j is introduced by randomly simulating $\phi^j_{mcs} \sim BETA(a,b)$ and setting $y^j_{mcs} = \tilde{y}^j_{mcs}$ and $x^j_{u,mcs} = \tilde{x}^j_{u,mcs} / (1 - \phi^j_{mcs})$ for u =

1, …, U [xii]. For each simulation repetition *mcs*, the generated reference data $x_{u,mcs}^{j}$ and y_{mcs}^{j} was used to populate an N by U input matrix $X_{N,mcs}$ and an N by 1 output matrix $Y_{N,mcs}$.

Estimated Convergence Rate and Normality Test Results

We completed the above process for a number of input U numbers and quantile levels α. Due to space limitations, we discuss results using the CRS and VRS BETA(1,3), BETA(2,4), and BETA(5,10) DGP with V = 1 output, U = 1, 3, or 5 inputs, and α = 0.95. Figure 5 presents panel plots demonstrating several results for the VRS-BETA(1,3) DGP with U = 3 inputs. The upper left panel presents a boxplot of the estimated qeffhat = $\hat{\phi}_{m_i}^{0.95}$ values by sample size. The boxplot demonstrates that: (1) the dispersion of the $\hat{\phi}_{m_i}^{0.95}$ estimates decrease with sample size, (2) the median values of the $\hat{\phi}_{m_i}^{0.95}$ estimates increase with sample size, and (3) the median values appear to be convergent with increases in sample size. For all DGP examined we obtained similar results indicating that the $\hat{\phi}^{\alpha}$ estimator is apparently a biased but convergent estimator as sample size increases. The bias result is not troubling in that the nCm bootstrapping process can be used to obtain bias-corrected estimates for $\hat{\phi}^{\alpha}$ (Politis, et. al)[xiii].

The upper right panel in figure 5 presents a boxplot of the log of the inter-quantile-ranges (iqnr) (generated in the convergence rate estimation process) plotted against the log of the sample sizes. An examination of the second boxplot indicates that log(iqnr) visually appears to decrease linearly with log(m). For this example, when log(iqnr) is regressed against log(m), the resulting slope parameter is -0.505 giving convergence rate estimate $\hat{\beta}$ = 0.505 as presented in table 2.

The lower panels in figure 5 present qqnorm-qqline plots for the 1000 $\hat{\phi}_{1000,mcs}^{0.95}$ and $\hat{\phi}_{20000,mcs}^{0.95}$ estimates. An examination of the plots provides strong evidence that the $\hat{\phi}_{m_i,mcs}^{0.95}$ estimates are normally distributed. When Pearson's normality test is applied to the residuals, the resulting p-values, presented in table 2, are 0.527, and 0.146, indicating that normality cannot be rejected for the $\hat{\phi}_{1000,mcs}^{0.95}$ and $\hat{\phi}_{20000,mcs}^{0.95}$ estimates.

Table 2 presents the large sample $\hat{\beta}$ convergence rate estimates and normality test p-values for the BETA(1,3), BETA(2,4), and BETA(5,10) data generating processes with constant and variable returns to scale and number of inputs U = 1, 3, and 5. In table 2, the estimated convergence rates $\hat{\beta}$ are close to 0.5 for all DGP, returns to scale, and number of input levels U examined. The Pearson p-values indicate that normality of $\hat{\phi}_{m_i}^{0.95}$ is not rejected with 7 of 180 or 3.9% of the p-values being below 0.05.

Figure 5: Panel Plots of Large Sample Parameter Estimates by Sample Size, Log(iqnr) by Log(Sample Size), and qqnorm Plots of Parameter Estimates by Sample Size for VRS-BETA(1,3)-U3 Data Generating Process

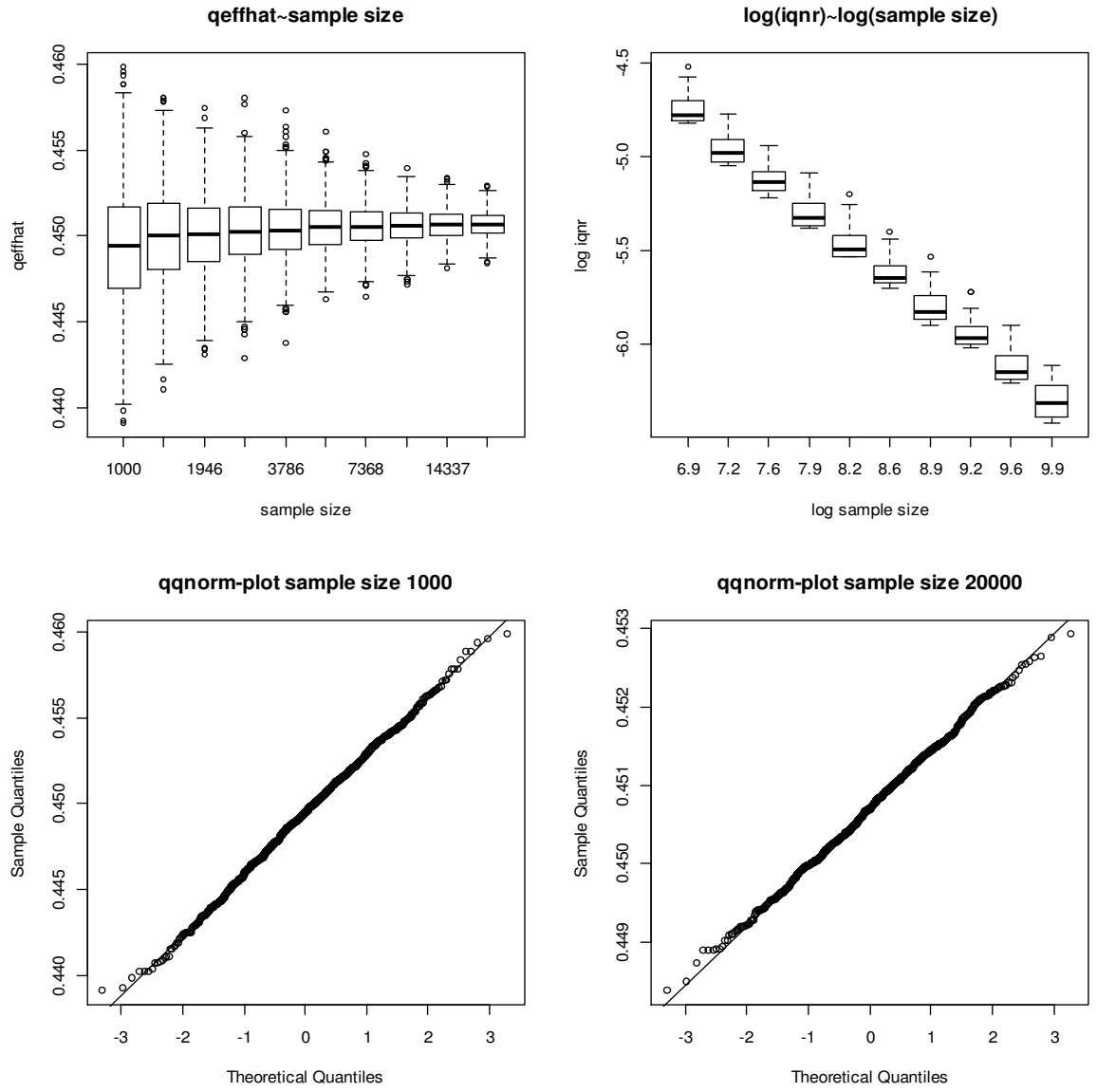

Table 2 : Large Sample Convergence Rate Estimates and Pearson-Normality-Test P-Values by DGP, RTS, Number of Inputs U, and Sample Size

				PEARSON NORMALITY TEST P-VALS BY SAMPLE SIZE									
DGP	RTS	U	$\hat{\beta}$	m1000	m1395	m1946	m2714	m3786	m5282	m7368	m10278	m14337	m20000
BETA13	CRS	1	0.525	0.057	0.131	0.164	0.114	0.436	0.198	0.200	0.452	0.323	0.361
BETA13	CRS	3	0.506	0.355	0.827	0.980	0.188	0.857	0.426	0.343	0.423	0.005	0.206
BETA13	CRS	5	0.522	0.781	0.729	0.420	0.108	0.111	0.486	0.364	0.894	0.674	0.262
BETA13	VRS	1	0.500	0.530	0.684	0.852	0.370	0.738	0.469	0.647	0.499	0.792	0.835
BETA13	VRS	3	0.505	0.527	0.496	0.126	0.817	0.873	0.697	0.355	0.967	0.582	0.146
BETA13	VRS	5	0.513	0.094	0.857	0.803	0.061	0.436	0.346	0.751	0.547	0.111	0.423
BETA24	CRS	1	0.491	0.869	0.131	0.798	0.003	0.978	0.376	0.564	0.657	0.089	0.019
BETA24	CRS	3	0.491	0.884	0.066	0.433	0.575	0.880	0.267	0.103	0.923	0.924	0.506
BETA24	CRS	5	0.498	0.021	0.533	0.729	0.370	0.589	0.204	0.089	0.674	0.052	0.456
BETA24	VRS	1	0.516	0.589	0.650	0.864	0.684	0.726	0.394	0.410	0.585	0.160	0.328
BETA24	VRS	3	0.502	0.558	0.732	0.976	0.994	0.833	0.099	0.190	0.080	0.551	0.097
BETA24	VRS	5	0.503	0.042	0.257	0.394	0.866	0.285	0.213	0.097	0.151	0.056	0.379
BETA510	CRS	1	0.494	0.564	0.039	0.456	0.778	0.916	0.312	0.803	0.544	0.373	0.713
BETA510	CRS	3	0.491	0.086	0.896	0.222	0.413	0.852	0.544	0.095	0.869	0.317	0.690
BETA510	CRS	5	0.508	0.719	0.397	0.254	0.169	0.063	0.674	0.795	0.065	0.738	0.806
BETA510	VRS	1	0.487	0.838	0.911	0.789	0.857	0.997	0.171	0.249	0.509	0.370	0.482
BETA510	VRS	3	0.494	0.931	0.388	0.987	0.909	0.571	0.238	0.664	0.527	0.582	0.267
BETA510	VRS	5	0.501	0.707	0.869	0.025	0.985	0.070	0.472	0.943	0.122	0.602	0.252

We utilized the "large sample" β estimation process with a number of other assumed DGP including DGP with different ranges for X and Y, various returns to scale, and multiple inputs and multiple outputs. Convergence rate estimates and normality test results similar to those reported in Table 2 were obtained for all DGP examined to date. As a robustness check of our convergence rate estimation process, we used the same procedures and DGP to estimate large sample convergence rates for the order-α FDH estimator. The order-α estimator has a known asymptotic convergence rate (root-n) and parameter distribution (normal) (Simar and Wilson (2011-a)). In the order-α case, our "large sample" results indicate order-α root-n convergence and large sample normality for all DGP examined.

We conclude this section, however, by reminding the reader that we have not been able to derive closed form expressions for either the root-n convergence rate or the asymptotic normality of the qDEA estimator. We also emphasize that, as $\alpha \to 1$ or $q \to 0$, the convergence rates for both the qDEA and order-α estimators will approach the convergence rates of the underlying DEA or

FDH processes. We are experimenting with the use of Politis et. al.'s (1999) and Geyer's finite-sample β estimation process in estimating convergence rates as $\alpha \to 1$ and β diverges from 1/2.

8. Summary, Caveats, and Conclusions

This paper has presented procedures for estimating more robust DEA distance metrics by allowing up to a user-specified proportion of DMU data points to lie external to the qDEA-hyperplane. The qDEA procedures are applicable with most LP based estimation procedures and can be implemented using standard linear programming software thereby accommodating LP's ability to incorporate alternative return-to-scale assumptions and identify or impose input-output price information. Monte Carlo simulations indicate that qDEA distance estimates appear to exhibit root-n convergence and large sample normality.

However, that as $\alpha \to 1$ or $q \to 0$, the convergence rates β and the distribution of the $\hat{\phi}^{\alpha}$ estimates for both the qDEA and order-α estimators will approach the convergence rates and distributions of the underlying DEA or FDH processes. In situations where the researcher uses qDEA to identify and eliminate a relatively small number of outliers, we suggest that the researcher assume the convergence rate of the underlying DEA process and estimate confidence intervals using empirical quantiles. We also remind the reader that, while we have obtained results similar to those reported above for all DGP examined to date, we have not derived closed forms expressions for the asymptotic properties of the qDEA-α estimator.

We note that, in our experience, the analyst will find an increased incidence of "superefficient-infeasible" solutions in some directions with VRS for DMU's that are qDEA-α superefficient. Several approaches are available if the analyst wishes to obtain distance metrics for these DMUs. We refer the reader to the relevant literature should this be a concern.

We conclude by noting that qDEA should prove useful in estimating more robust DEA distance metrics. We also believe that qDEA will prove to be particularly useful in regulatory and benchmarking applications in that qDEA directly accommodates the estimation of quantile-based distance metrics while endogenously allowing proportions or quantiles (such as the top one, five or ten percent) of DMU's to lie external to the resulting hyperplanes. Quantile-DEA provides a useful mechanism whereby a decision-maker or researcher can obtain information about the practical "reachability" of projected points by exploring the interior of the "feasible" production technology

and the identifying the proportion of DMUs that have been able to reach or exceed a qDEA performance metric. The qDEA allows the user to directly "slice the onion" of the DEA revealed technology to the desired quantile depth using conventional LP-based procedures.

---

[i] In the following discussion, the notation ϕ denotes the conventional DDEA distance for DMU-0, ϕ^{α} denotes DMU-0's directional distance to the qDEA-α hyperplane estimated while allowing up to proportion q = 1-α of the reference set's input-output observations to lie outside the qDEA-α hyperplane, and $\phi^{j,\alpha}$ denotes the qDEA-α distance for DMU j. The notation $\hat{\phi}_n$, $\hat{\phi}_n^{\alpha}$, and $\hat{\phi}_n^{j,\alpha}$ denotes distances estimated using a sample of size n.

[ii] Rockafellar and Urysev (2000) presented a linear programming model that minimized the upside or loss-risk cVaR_q while endogenously identifying the cVaR_q's associated VaR_q level. Their objection function is equivalent to minimizing $t + \frac{1}{q}\rho_{UPM}(t) = \mathrm{cVaR}_q(t)$ with $t = \mathrm{VaR}_q$. Rockafellar and Urysev's model can be modified to optimize an objective function subject to a maximal cVaR_q by imposing the constraint $t + \frac{1}{q}\rho_{UPM}(t) \le g$ which is equivalent to the UPM constraint derived previously (8).

[iii] The $\tilde{t} = \mathrm{VaR}_q$ and $g = \mathrm{cVaR}_q$ results can easily be demonstrated for system (9). System (9) searches over potential portfolios while endogenously identifying the $\tilde{t}$ level associated with the least conservative or minimal level of the probability limit $\frac{\rho_{LPM}(t)}{t-g}$. Note that $\rho_{LPM}(t) = \int_{-\infty}^{t}(t-x)\,f(x)\,dx = F(t)[t - E\{x \mid x \le t\}]$ and $\frac{d}{dt}\rho_{LPM}(t) = F(t)$. Taking the derivative of the linear LPM probability bound with respect to t and setting the result equal to zero gives:

$$\frac{d}{dt}\frac{\rho_{LPM}(t)}{(t-g)} = \frac{F(t)(t-g) - \rho_{LPM}(t)}{(t-g)^2} = \frac{F(t)(t-g) - F(t)[t - E\{x \mid x \le t\}]}{(t-g)^2} = 0 \Leftrightarrow g = E\{x \mid x \le \tilde{t}\}$$

with the second derivative of $\frac{\rho_{LPM}(t)}{t-g}$ with respect to t (evaluated at the minimal $\tilde{t}$) being strictly positive..

Assuming the sufficiency constraint is binding i.e. $\tilde{t} - \frac{1}{q}\rho_{LPM}(\tilde{t}) = g$ implies:

$$\rho_{LPM}(\tilde{t}) = q(\tilde{t} - g) \Rightarrow F(\tilde{t})[\tilde{t} - E\{x \mid x \le \tilde{t}\}] = q(\tilde{t} - g) \Leftrightarrow F(\tilde{t}) = q\,.$$

Thus, with AWHH's downside risk constraint $t - \frac{1}{q}\rho_{LPM}(t) \ge g$, the endogenously selected $\tilde{t}$ level is the $\mathrm{VaR}_q(\tilde{x})$ of the optimal portfolio's income $\tilde{x}$ such that $\mathrm{Prob}(\tilde{x} \le \tilde{t}) = q$ and *g* is the associated $\mathrm{cVaR}_q(\tilde{x})$ or the $\mathrm{Expected}\{\tilde{x} \mid \tilde{x} \le \tilde{t}\}$.

[iv] System (9) is more broadly applicable than AWHH's or RU's chance-constrained or cVaR constrained setting in that the $y_{k,j}$ values need not be in monetary or rates of return units and the model need not involve "risk". System (9) can be generalized to other classes of linear programming models where the researcher desires to allow up to a proportion of endogenously identified constraints to be violated. In this paper, we utilize similar constraints in a DDEA model that allows a proportion of endogenously identified input/output points to lie external to the q-DEA hyperplane.

[v] We use the terminology "support points" to denote the points that define the hyperplane onto which the given DMU's input-output points are projected with ϕ^{α} being the distance from the initial point to the projected point on the hyperplane.

[vi] The qDEA stage 1 solution is conservative in that its projected $(\hat{x}, \hat{y})$ values are projected from the two potential external points B and E as well as point D in figure 1. This is apparent by examining the LP's dual values presented in figure 3. Thease dual values are DMU projection weights in dual system (10)'s associated primal LP.

[vii] As discussed below, the solution to the continuous LP in system (10) will often be conservative in that fewer than proportion q of the DMU's may lie external to the qDEA-α hyperplane. We initially experimented with an exact mixed binary model:

$\min_{p,w,\delta} -y_0 \bullet p + x_0 \bullet w \quad st.\ Y \bullet p - X \bullet w - M \bullet \delta \le 0;\ d_y^0 \bullet p + d_x^0 \bullet w = 1;\ \sum_{i=1}^{n} 1/n\, \delta_j \le q;\ p \ge 0;\ w \ge 0;$ and $\delta_j = 0,1$ where p and w are continuous choice vectors, Y and X are input and output matrices, M is a diagonal matrix with "large" positive values on the diagonal and δ is a binary zero-one vector. While the mixed binary model gave exact solutions when it could be solved, the current state of mixed binary model algorithms limits its applicability in qDEA due to the prohibitive amounts of time required to obtain solutions – especially when bootstrapping is desired.

[viii] For firms with positive levels of all input and outputs, the "worst-case-reference point" procedure discussed by Atwood, Shaik, and Walden (2017) quickly identifies such a feasible movement direction for any DMU. A worst case reference point is can be computed as $\left(x_u^{wc}, y_v^{wc}\right)$ where $x_u^{wc} = \max\left(\max_j\left(x_u^j\right), x_u^0\right)$ and $y_v^{wc} = \min\left(\min_j\left(y_v^j\right), y_v^0\right)$. A feasible direction $\left(d_u^0, d_v^0\right)$ can be computed as $\left(d_u^0, d_v^0\right) = \left(x_u^{wc} - x_u^0,\ y_v^0 - y_v^{wc}\right)$. For qDEA-$\alpha$ superefficient firms, the estimated distance $\hat{\phi}^{\alpha}$ in expression (1) will be negative but a feasible projection point $\left(\tilde{x}^0, \tilde{y}^0\right) = \left(x^0 - \hat{\phi}^{\alpha}\, dx^0, y^0 + \hat{\phi}^{\alpha}\, dy^0\right)$ on DMU-0's qDEA-α hyperplane can always be found. For DMU's with zero levels for some inputs or outputs see the discussion by Lee, Chu, and Zhu (2012).

[ix] More formally m(n) << n denotes using a rule for selecting m (as a function on n) such that $\underset{n\to\infty}{Lim}\, m(n) = \infty$ and $\underset{n\to\infty}{Lim} \frac{m(n)}{n} = 0$. One such rule is to set $m(n) = K\sqrt{n}$ where K is a positive scalar.

[x] The DEA CRS and VRS convergence rates are, respectively, $\beta = \frac{2}{U+V}$ and $\beta = \frac{2}{U+V+1}$. The FDH, order-m, and order-α convergence rates are, respectively, $\beta = \frac{1}{U+V}$, $\beta = 1/2$, and $\beta = 1/2$ (Simar, L. and P. Wilson. (2011-a))

[xi] Geyer used logs in creating a set of m_i values to obtain more aesthetically pleasing log-log plots. We also use logs to decrease computation times while still spanning the subsample size range, (1000, 20000).

[xii] With an input orientation DDEA model and DDEA distance ϕ, the "efficient" projected point is $\tilde{x} = x - \phi x = (1-\phi)x \Rightarrow x = \tilde{x}/(1-\phi)$ with $0 \le \phi < 1$. Simar and Wilson (2011-b) introduced input inefficiency by generating $\tau \sim EXP(3)$ and setting $x = \tilde{x}e^{\tau}$. If $\frac{1}{(1-\phi)} = e^{\tau}$, it is a relatively easy exercise to show that

$\phi \sim BETA(1,3)$ when $\tau \sim EXP(3)$. Generating $\phi^j \sim BETA(a,b)$ rather than using an exponential distribution allowed us greater flexibility in generating sets of ϕ^j values with fewer or more points near the "efficient" $\phi = 0$ boundary in our sets of Monte Carlo simulations.

[xiii] While not reported in this paper due to space limitations, we have conducted a number of nCm subsample confidence interval testing exercises similar to those reported by Simar and Wilson (2011-b). Confidence interval coverage levels similar to those reported by Simar and Wilson (2011-b) were obtained for nCm bootstrapped qDEA estimates.

References

Adler, N., Liebert, V., and Yazhemsky, E. (2013). "Benchmarking airports from a managerial perspective". *Omega. 41* (2), 442–458.

Anthonisz, S. (2012). "Asset pricing with partial-moments." *Journal of Banking & Finance.* 36, 2122–2135.

Aparicio, J., and Pastor, J. (2014). "Closest targets and strong monotonicity on the strongly efficient frontier in DEA". *Omega.* 44, 51–57.

Aparicio, J., Cordero, J., and Pastor, J. (2017). "The determination of the least distance to the strongly efficient frontier in data envelopment analysis oriented models: modelling and computational aspects". *Omega.* 71, 1–10.

Aparicio, J., Ruiz, J., and Sirvent, I. (2007). "Closest targets and minimum distance to the Pareto-efficient frontier in DEA". *Journal of Productivity Analysis.* 28 (3), 209–218.

Aragon, Y., Daouia, A., and Thomas-Agnan, C. (2005). "Nonparametric frontier estimation: A conditional quantile-based approach". *Econometric Theory.* 21(2), 358-389.

Atwood, J. (1985). "Demonstration of the use of lower partial moments to improve safety-first probability limits". *American Journal of Agricultural Economics.* 67, 787-93.

Atwood, J., and Shaik, S. (2018) "Quantile DEA: estimating qDEA-alpha efficiency estimates with conventional linear programming." *Productivity and Inequality.* Springer Press. New York.

Atwood, J., Shaik. S. and J. Walden. (2017) "Radial efficiency metrics using worst-case reference points." *15th European Workshop on Efficiency and Productivity Analysis. (EWEPA).* London. June, 12-15.

Atwood, J., Watts, M., Helmers, G., and Held, L. (1988). "Incorporating safety-first constraints in linear programming production models." *Western Journal of Agricultural Economics.* 13, 29-36.

Banker, R., Førsund. F., and Zhang, D. (2017). "Use of data envelopment analysis for incentive regulation of electric distribution firms". *Data Envelopment Analysis Journal.* Vol. 3(1–2), 1-47.

Barr, R., Durchholz, M., and Seiford, L. (2000). "Peeling the DEA onion: layering and rank-ordering DMUs using tiered DEA". Southern Methodist University Technical Report.

Bawa, V. (1975). "Optimal rules for ordering uncertain prospects". *Journal of Financial Economics.* 2(1), 95–121.

Bawa, V., and E. Lindenberg. (1977). "Capital market equilibrium in a mean-lower partial moment framework". *Journal of Financial Economics.* 5(1977), 189-200.

Berck, P., and Hihn, J. (1982). "Using the semivariance to estimate safety-first rules." *American Journal of Agricultural Economics*. 64, 298-300.

Bogetoft, P. (2012). *Performance Benchmarking: Measuring and Managing Performance.* Springer. New York.

Bogetoft, P., and Otto, L. (2011). *Benchmarking with DEA, SFA, and R.* Springer. New York.

Bottasso. A., and Conti, A. (2011). *Quantitative Techniques for Regulatory Benchmarking - A CERRE Study*. CERRE. Brussels.

Boxwell, R. (1994). *Benchmarking for Competitive Advantage*. McGraw-Hill, New York, NY.

Cazals, C., Florens, J., and Simar, L. (2002). "Nonparametric frontier estimation: a robust approach", *J. Econometrics*. 106, 1–25.

Chambers, G., Chung, Y., and Färe. R. (1996), "Benefit and distance functions". *Journal of Economic Theory.* 70, 407–419.

Charnes, A., Cooper, W., and Rhodes, E. (1978). "Measuring the efficiency of decision making units." *European Journal of Operational Research.* 2, 429-444.

Chen, Y. (2005). "Measuring super-efficiency in DEA in the presence of infeasibility". *European Journal of Operational Research*. 161, 545–551.

Chen, Y., and Liang, L. (2011). "Super-efficiency DEA in the presence of infeasibility: One model approach". *European Journal of Operational Research.* 213, 359–360.

Cook, W., Liang, L., Zha, Y., and Zhu, J. (2009). "A modified super-efficiency DEA model for infeasibility". *Journal of Operational Research Society*. 60, 276–281.

Cook, W., Ruiz, J., Sirvent, I., and Zhu, J. (2017). "Within-group common benchmarking using DEA." *European Journal of Operational Research.* 256, 901-910.

Cooper, W., Seiford, L., and Tone, K., 2006. *Introduction to Data Envelopment Analysis and Its Uses.* Springer. NewYork.

Cumova, D. and D. Nawrocki. (2014). "Portfolio optimization in an upside potential and downside risk framework". *Journal of Economics and Business.* 71, 68-89.

Dai, X., and Kuosmanen, T. (2014). "Best-practice benchmarking using clustering methods: Application to energy regulation". *Omega. 42* (1), 179–188.

Daouia, A., and Simar, L. (2005). "Robust nonparametric estimators of monotone boundaries". *Journal of Multivariate Analysis* 96, 311–331.

Daouia, A. and Simar, L. (2007). "Nonparametric efficiency analysis: a multivariate conditional quantile approach." *Journal of Econometrics*. 140, 375-400.

Daraio, C. and Simar, L. (2007). *Advanced Robust and Nonparametric Methods in Efficiency Analysis*. Springer. New York.

Fishburn, P. (1972). "Mean-risk analysis with risk associated with below-target returns." *American Economic Review*. 67, 116-26.

Geyer, C. (2013). "Statistics 5601 Notes: The Subsampling Bootstrap." University of Minnesota. Reference Material. //www.stat.umn.edu/geyer/5601/examp/subboot.html.

Lee, H., Chu, C., and Zhu, J.. (2011). "Super-efficiency DEA in the presence of infeasibility". *European Journal of Operational Research*. 212, 141–147.

Lee, H., Chu, C., and Zhu, J. (2012). "Super-efficiency infeasibility and zero data in DEA". *European Journal of Operational Research*. 216, 429-433.

Lovell, C., and Rouse, A. (2003). "Equivalent standard DEA models to provide superefficiency scores". *Journal of the Operational Research Society*. 54(1), 101–108.

Markowitz, H. (1952). "Portfolio Selection". *The Journal of Finance.* 7(1), 77–91.

Nawrocki, D. (1991). "Optimal algorithms and lower partial moment: ex post results". *Applied Economics*. 23(3), 465-470.

Politis, D., Romano, J., and Wolf, M. (1999). *Subsampling*. Springer. New York.

Politis, D., Romano, J., and Wolf, M. (2001). "On the asymptotic theory of subsampling." *Statistica Sinica.* 11, 1105-1124.

Risk Management Association (2019). *Annual Statement Studies – Financial Ratio Benchmarks, Volume I 2017-2018.* https://www.rmahq.org/uploadedFiles/Knowledge_Center/Publications_and_Tools/Statement_Studies/2017-18%20FRB%20Definition%20of%20Ratios.pdf

Ramón, N., Ruiz, J., and Sirvent, I. (2018). "Two-step benchmarking: Setting more realistically achievable targets in DEA". *Expert Systems With Applications*. 92, 124–131.

Rockafellar, R., and Uryasev, S. (2000). "Optimization of conditional value-at-risk". *Journal of Risk.* 2, 21–41.

Ruiz, J. and Sirvent, I. (2016). "Common benchmarking and ranking of units with DEA". *Omega.* 65, 1–9 .

Seiford, L., and Zhu, J. (1999). "Infeasibility of super-efficiency data envelopment analysis models". *INFOR* 37(May), 174–187.

Simar, L. 2003. "Detecting outliers in frontier models: a simple approach." *Journal of Productivity Analysis.* 20, 391-424.

Simar, L., and Wilson, P. (2011-a). "Estimation and inference in nonparametric frontier models: recent developments and perspectives." *Foundations and Trends in Econometrics*. 5(3–4), 183–337.

Simar, L., and Wilson, P. (2011-b). "Inference by the m out of n bootstrap in nonparametric frontier models." *Journal of Productivity Analysis.* 36, 33-53.

Wheelock, C., and Wilson, P. (2008). "Non-parametric, unconditional quantile estimation for efficiency analysis with an application to Federal Reserve check processing operations". *Journal of Econometrics.* 145, 209–225.

Wilson, P. (1993). "Detecting outliers in deterministic nonparametric frontier models with multiple outputs". *Journal of Business and Economic Statistics.* 11, 319–323.

Wilson, P. (1995). "Detecting influential observations in data envelopment analysis". *Journal of Productivity Analysis.* 6, 27–45.

Zanella, A., Camanho, A., and Dias, T. (2013). "Benchmarking countries' environmental performance". *Journal of the Operational Research Society.* 64 (3), 426–438.

Zhu. S., D. Li, and S. Wang. (2009). "Robust portfolio selection under downside risk measures". *Quantitative Finance*. 9(7), 869-885.

Appendix

The results of the qDEA process described in the main body of the paper will frequently be conservative in that fewer than proportion *q* of the observed data points will lie exterior to the estimated qDEA hyperplane at the completion of the second stage of the qDEA process. A detailed discussion of the reason for the conservativeness is beyond the scope of the paper but the problem results from the use of the stochastic inequality when endogenously contorting the augmented qDEA stage I problem. This appendix presents an example that demonstrates the potential conservativeness of the qDEA stage 2 solution and an iterative process designed to obtain less conservative solutions if desired by the researcher.

Figure A1 plots data from the main body's example but with firm B's data modified to a more extremal $\left(x^B, y^B\right) = (2,5)$. Figure A1 plots the data points and the qDEA-1, qDEA-7/8, and qDEA-6/8 CRS hyperplanes for the revised problem. Note that when two points are allowed to lie external to the qDEA-6/8 hyperplane, the projected points should lie on the blue ray defined by the origin and point D with points B and E lying external to the qDEA-6/8 hyperplane.

Figures A2 and A3 present the qDEA Stage-1 and Stage-2 tableaus for the first iteration of the modified problem. These tableaus have been modified by adding a column "LHS-External" that indicates whether the LP solution's left-hand-side exceeds zero (i.e. the corresponding DMU is external to the qDEA hyperplane). The results presented in figure A2 indicate that the qDEA stage 1 model has identified two *potential* external points i.e. points A and B. However, when the associated constraints are relaxed in qDEA-stage 2, the results presented in figure A3 indicates that only point B (with a "left-hand-side" value exceeding 0) actually lies external to the estimated hyperplane. We note that the resulting distance estimate is 0.7778 which is identical to the qDEA-7/8 distance reported for DMU H in the main body's table 1. Although space prevents a complete discussion, we have run a number of simulations obtaining similar results i.e. when using one iteration of qDEA, the estimated distance $\hat{\phi}^{\hat{\alpha}}$,with $\hat{\alpha} = 1 - \hat{q}$ and $\hat{q}$ the

actual proportion of points external to the estimated qDEA hyperplane, appears to be a convergent and normally distributed estimate of the distance to the qDEA-$\hat{\alpha}$ hyperplane.

In figures A2 and A3, we have referred to the first round of conventional qDEA process as Iteration-1. Figures A3 and A4 illustrate the process if the analyst wishes to complete additional iterations to reduce or eliminate the conservativeness of the qDEA Stage-2 results. In figure A4 (qDEA Stage-1 Iteration-2) we have relaxed the constraint of the qDEA stage-2 Iteration-1 external point (point B) by adding a "big-M" to the corresponding RHS location, indicated that we are searching for up to 1 additional external point, and resolved the problem. The results indicate that the model has identified point E as a potential additional external point. Figure A5 presents the qDEA Stage-2 Iteration-2 tableau where both the constraints from Stage-2 Iteration 1's actual external points (point B) and the qDEA Stage-1 Iteration-1's potential additional external points (point E) have been relaxed. The LP solution's results indicate that we have now identified two external points (points B and E) whose LHS values exceed zero. The resulting distance estimate is $\hat{\phi}^{H,6/8} = 0.5714$ which is identical to the qDEA-6/8 "one-one" distance for DMU H in table 1.

Since we have identified two external DMU's, our iterative process stops and returns the qDEA Stage-2 Iteration-2 results to the user. When estimating models containing more DMU's the process may require more iterations. R code available from the authors allows the user to specify the maximal number of iterations to be completed as well as specifying a $q - \hat{q}$ tolerance level where the iterative process is stopped if $q - \hat{q}$ falls below the set tolerance. The R code also returns the values for $\hat{q}$ i.e. the proportion of points actually external to the qDEA hyperplane.

Figure A1: Modified Cooper, Seiford, and Tones Single-Input Single Output Example with DDEA Directions and qDEA CRS Hyperplanes

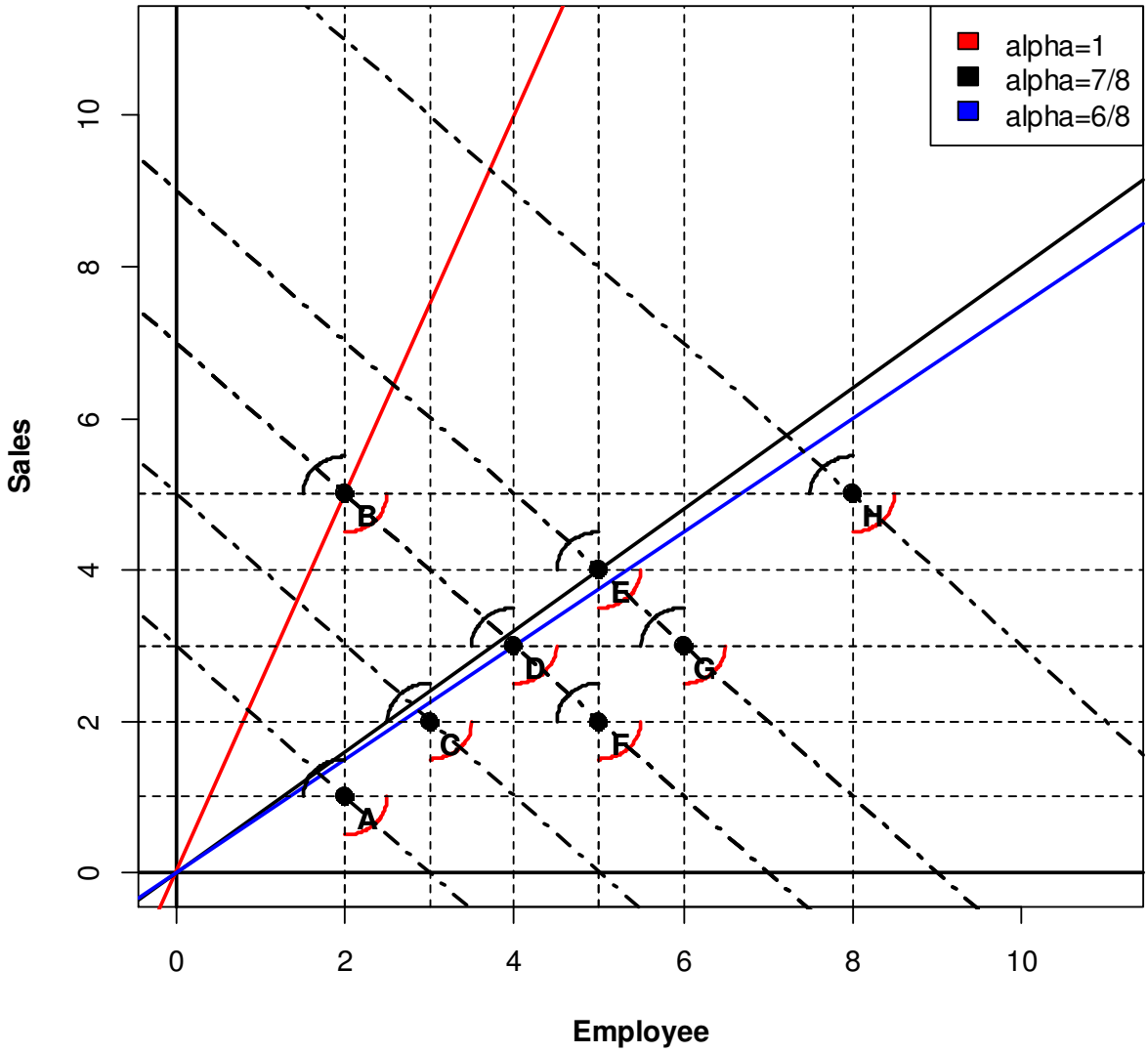

Figure A2: Modified qDEA-6/8 Stage-1 Iteration-1 Tableau Identifying Two Potential External Points

qDEA STAGE-1 ITERATION-1

MODIFIED CST EXAMPLE			SELECTED			N out =	2									
DUAL PROBLEM			DMU =	H		*q* =	0.37499									
																LHS
DMU	OUTPUT	INPUT	T	D-A	D-B	D-C	D-D	D-E	D-F	D-G	D-H	T-LPM		LHS	SIGN	RHS	External
A	1	-2	-1	-1	0	0	0	0	0	0	0	0		0.00000	<=	0	0
B	5	-2	-1	0	-1	0	0	0	0	0	0	0		0.00000	<=	0	0
C	2	-3	-1	0	0	-1	0	0	0	0	0	0		0.00000	<=	0	0
D	3	-4	-1	0	0	0	-1	0	0	0	0	0		-0.06667	<=	0	0
E	4	-5	-1	0	0	0	0	-1	0	0	0	0		-0.13335	<=	0	0
F	2	-5	-1	0	0	0	0	0	-1	0	0	0		-1.06667	<=	0	0
G	3	-6	-1	0	0	0	0	0	0	-1	0	0		-1.13335	<=	0	0
H	5	-8	-1	0	0	0	0	0	0	0	-1	0		-1.26670	<=	0	0
DIRECTION	1	1	0	0	0	0	0	0	0	0	0	0		1.00000	==	1	
LPM CALC	0	0	0	0.125	0.125	0.125	0.125	0.125	0.125	0.125	0.125	-1		0.00000	==	0	
QRESTRICT	0	0	1	0	0	0	0	0	0	0	0	2.6667		0.00000	<=	0	
OBJ	-5	8	0	0	0	0	0	0	0	0	0	0		1.93338	<--minOBJ		

NOTE THIS OBJ IS NOT THE FINAL ANSWER
STAGE 2 PROVIDES THE FINAL ANSWER

t-lower bound -1000

													PROJECTED POINTS	
	P	W	T	D-A	D-B	D-C	D-D	D-E	D-F	D-G	D-H	T-LPM	$\tilde{x}$	$\tilde{y}$
SOLUTION	0.46666	0.53334	-0.6667	0.0667	1.9333	0	0	0	0	0	0	0.25	6.0666	6.9334

# POTENTIAL Stage 2			Potential qDEA Stage-2 Phase-1 External Points							
POINTS OUT HULL =	2		1	1	0	0	0	0	0	0

Figure A3: Modified qDEA-6/8 Stage-2 Iteration-1 Tableau

	qDEA STAGE-2 ITERATION-1						
MODIFIED CST EXAMPLE			SELECTED				
DUAL PROBLEM			DMU =	H			
							LHS
DMU	OUTPUT	INPUT		LHS	SIGN	RHS	EXTERNAL
A	1	-2		-0.3333	<=	1000	0
B	5	-2		1.8889	<=	1000	1
C	2	-3		-0.2222	<=	0	0
D	3	-4		-0.1111	<=	0	0
E	4	-5		0.0000	<=	0	0
F	2	-5		-1.1111	<=	0	0
G	3	-6		-1.0000	<=	0	0
H	5	-8		-0.7778	<=	0	0
DIRECTION	1	1		1	==	1	TOTAL EXT
OBJ	-5	8		0.7778	<--minOBJ		1
				PROJECTED POINTS			
	P	W		$\tilde{x}$	$\tilde{y}$		
SOLUTION	0.555556	0.444444		7.2222	5.7778		

Figure A4: Modified qDEA-6/8 Stage-1 Iteration-2 Tableau Identifying Additional Potential External Points

qDEA STAGE-1 ITERATION-2

MODIFIED CST EXAMPLE | SELECTED | Additional N out = 1

DUAL PROBLEM | DMU = H | q = 0.24999

DMU	OUTPUT	INPUT	T	D-A	D-B	D-C	D-D	D-E	D-F	D-G	D-H	T-LPM		LHS	SIGN	RHS	LHS External
A	1	-2	-1	-1	0	0	0	0	0	0	0	0		-0.25000	<=	0	0
B	5	-2	-1	0	-1	0	0	0	0	0	0	0		2.00000	<=	1000	1
C	2	-3	-1	0	0	-1	0	0	0	0	0	0		-0.12500	<=	0	0
D	3	-4	-1	0	0	0	-1	0	0	0	0	0		0.00000	<=	0	0
E	4	-5	-1	0	0	0	0	-1	0	0	0	0		0.00000	<=	0	0
F	2	-5	-1	0	0	0	0	0	-1	0	0	0		-1.00000	<=	0	0
G	3	-6	-1	0	0	0	0	0	0	-1	0	0		-0.87500	<=	0	0
H	5	-8	-1	0	0	0	0	0	0	0	-1	0		-0.62500	<=	0	0
DIRECTION	1	1	0	0	0	0	0	0	0	0	0	0		1.00000	==	1	0
LPM CALC	0	0	0	0.125	0.125	0.125	0.125	0.125	0.125	0.125	0.125	-1		0.00000	==	0	0
QRESTRICT	0	0	1	0	0	0	0	0	0	0	0	4.0002		0.00000	<=	0	0
OBJ	-5	8	0	0	0	0	0	0	0	0	0	0		0.687504	<--minOBJ		

NOTE THIS OBJ IS NOT THE FINAL ANSWER

STAGE 2 PROVIDES THE FINAL ANSWER

t-lower bound -1000

	P	W	T	D-A	D-B	D-C	D-D	D-E	D-F	D-G	D-H	T-LPM
SOLUTION	0.5625	0.4375	-0.0625	0	0	0	0	0.125	0	0	0	0.0156

PROJECTED POINTS	
$\tilde{x}$	$\tilde{y}$
7.3125	5.6875

ADDITIONAL POTENTIAL Stage 2

POINTS OUT HULL = 1

Potential Additional qDEA Stage-2 Phase-2 External Points							
0	0	0	0	1	0	0	0

Figure A5: Modified qDEA Stage-2 Iteration-2 Tableau

							LHS
DMU	OUTPUT	INPUT		LHS	SIGN	RHS	External
A	1	-2		-0.2857	<=	0	0
B	5	-2		2.0000	<=	1000	1
C	2	-3		-0.1429	<=	0	0
D	3	-4		0.0000	<=	0	0
E	4	-5		0.1429	<=	1000	1
F	2	-5		-1.0000	<=	0	0
G	3	-6		-0.8571	<=	0	0
H	5	-8		-0.5714	<=	0	0
DIRECTION	1	1		1	==	1	TOTAL EXT
OBJ	-5	8		0.5714	<--minOBJ		2
				PROJECTED POINTS			
	P	W		$\tilde{x}$	$\tilde{y}$		
SOLUTION	0.571429	0.428571		7.4286	5.5714		